

## Domain Size and Fluctuations at Domain Interfaces in Lipid Mixtures

*Heiko M. Seeger, Matthias Fidorra, Thomas Heimburg\**

Niels Bohr Institute, University of Copenhagen, Blegdamsvej 17, 2100 Copenhagen Ø, Denmark, and Max-Planck Institute for Biophysical Chemistry, 37077 Göttingen, Germany  
E-mail: theimbu@nbi.dk

**Summary:** Biomembranes consist of a complex mixture of a large number of lipids and proteins. In such mixtures, microscopic domains and macroscopically separated phases may exist. Here, we discuss phase behavior and domains formation of binary lipid mixtures. We show that the domain formation is accompanied by large fluctuations at the domain boundaries, resulting in altered physical properties at the boundaries, for instance in a pronounced increase of the elastic constants. Therefore, we argue that the physics of the membrane depends on the overall length scale of its domains interfaces. We present here confocal microscopy images, calorimetric melting profiles and Monte-Carlo simulations to understand the factors that determine domain formation, their sizes and the role of the domain interfaces.

**Keywords:** confocal microscopy; domains; elastic constants; fluctuations; phase diagrams

**Abbreviations:** DLPC - dilaureoyl phosphatidylcholine; DMPC – dimyristoyl phosphatidylcholine; DPPC - dipalmitoyl phosphatidylcholine; DSPC – distearoyl phosphatidylcholine

### Introduction

Biomembranes consist of a large variety of different lipids and proteins. The composition of each membrane is distinctively different, even between membranes of the various organelles within one cell [1]. About 80% of the lipids in eukaryotic membranes are zwitterionic phosphatidylcholines or phosphatidylethanolamines, the rest is uncharged or charged. Mitochondrial membranes, for instance, are rich in charged lipids (about one net negative charge per five lipid chains), whereas plasma membranes have typically less than one net negative charge per twenty lipid chains. Plasma membranes, on the other hand, are usually rich in cholesterol (up to 30% of the lipids), and there exist differences between inner and outer leaflets of the bilayers. The reason for the large diversity in lipid

composition is subject to an ongoing debate. In recent years it became increasingly evident that the lipid heterogeneity gives rise to domain formation in the membrane plane, which may influence diffusion pathways and communication networks between proteins and other molecules. More and more experimental data show the existence of domains in biomembranes, and that they are in fact important for membrane function. The finding of phase separation in lipid membranes is not at all new [2]. Domains were already visualized in monolayers in the 1980s [3]. First pictures of domains in vesicles, however, were published only 1999 in pioneering works by Koralch et al. [4], and by Bagatolli and Gratton [5]. In artificial lipid mixtures, domains are usually much larger and easier to observe with confocal microscopy than in intact biomembranes. In the biology community domains in biomembranes are frequently called “rafts”. Their sizes are typically below microscopic resolution and evidence for their existence is rather indirect. Many of those micro-domains seem to be rich in cholesterol, sphingolipids and special proteins [6]. However, it is not at all obvious that domains in biomembranes by necessity display a unique composition, and the finding of such specific domains may be artifacts from the preparation method, namely detergent extraction [7]. The term “raft” furthermore implies that they are often considered as stable functional units, comparable to large protein complexes.

The question arises whether the fact that domains in biomembranes are small is not in conflict with the assumption that they are rigid objects. In fact, in lipid mixtures fluctuations may be very large and the magnitude of fluctuations relates to the size of the fluctuating objects (relative fluctuations become larger for smaller objects). In some simple lipid systems macroscopic phase separation has been observed [8], meaning that the domain size is on the order of the vesicle size and the membrane demixes into just two macroscopic regions with distinctly different physical properties or order parameters. In such systems the domain size grows with vesicle size. In the thermodynamic limit, when a vesicle is infinitely large, the length and the physical properties of the domain interface can be neglected in relation to the overall features of the domains. Such macroscopic domains are called phases. The number of coexisting phases depends on the number of components and the number of degrees of freedom. The Gibbs phase rule applied to a system observed at constant pressure is given by

$$F = K - P + 1 \quad ,$$

where  $F$  is the number of degrees of freedom,  $K$  is the number of components ( $=2$  in a

binary lipid system in excess water) and  $P$  is the number of coexisting phases. In a binary system  $P$  may be 1, 2 or 3 (at eutectic or peritectic points). One complication in using Gibbs' phase rule is that a membrane may exhibit changes in curvature [8] and thus may display one more degree of freedom. Gibbs' phase rule was also derived neglecting phase boundaries, which can only be done if phase separation is macroscopic. Assuming macroscopic phase separation, one can use phase diagrams to calculate the relative fractions of each phase and their composition, making use of thermodynamic constructions, e.g. the lever rule [2]. The thermodynamic treatment becomes more complicated when domains are small and do not scale with system size. In the melting of a one-component membrane this case corresponds to a continuous transition (domains in the melting regime are smaller than system size and there is no latent heat) in contrast to a first order transition with macroscopic domain formation and latent heat [9]. In Monte-Carlo simulations one can distinguish first order melting from continuous transitions by analyzing histograms of the distribution of vesicular states. Continuous transitions display Gaussian fluctuations around the thermal equilibrium at all temperatures, whereas first order transitions display coexisting macroscopic states at the transition temperature [9]. In systems containing several components there also exists a fundamental difference between cases where domain sizes grow with system size as compared to cases where they are independent of scaling. In the second case, the properties of the domain interfaces can never be neglected and Gibbs' phase rule cannot adequately be applied.

This paper focuses on the factors that determine domain sizes, and where the differences between microscopic and macroscopic domain formation arise. To this purpose we compare heat capacity profiles with Monte-Carlo simulations and with Confocal Microscopy images that demonstrate domain formation in giant vesicles. In particular, we focus on the fluctuations at domain interfaces.

## Materials and Methods

Calorimetric experiments were performed using a Hart Scientific (Provo, Utah) four cell scanning calorimeter and a VP differential scanning calorimeter by MicroCal (Northampton, MA) using scan rates of 5 deg/hr. The lipid mixtures for calorimetry were dried from organic solvent (dichloromethane-methanol 2:1 mixtures). Samples were measured in distilled water at neutral pH or in a 10mM Hepes, 1mM EDTA buffer at pH 7.4. Vesicles for confocal microscopy were prepared on Indium Tin Oxide (ITO) cover

slips with the electroformation method [10]. The lipid mixtures for confocal microscopy (including a fraction of  $10^{-4}$  of fluorescence dyes specific for gel and fluid domains) were dried on the cover slip from organic solvent (dichloromethane-methanol 1:1 mixtures). Remaining solvent was removed in a high vacuum desiccator. The dry lipid films were hydrated and exposed to an alternating electrical field of 10 Hz and 3V [10]. Images were recorded using confocal microscopes by Leika and Zeiss.

The lipid melting behavior was modeled using Monte-Carlo simulations. Here, we employ an Ising-like two-state model, where each chain may be either in a gel state (ordered chains) or a fluid state (disordered chains). The two chain states are different in enthalpy and entropy. Furthermore, nearest neighbor interactions are defined that lead to interaction parameters, which are responsible for cooperative melting. In a two-component membrane, there are two states for each species, and 6 unlike nearest neighbor interactions. The Gibbs free energy of each configuration of such a system is given by:

$$G = n_A^f \cdot (\Delta H_A - T\Delta S_A) + n_B^f \cdot (\Delta H_B - T\Delta S_B) + n_{AA}^{gf} \omega_{AA}^{gf} + n_{AB}^{gg} \omega_{AB}^{gg} + n_{AB}^{gf} \omega_{AB}^{gf} + n_{AB}^{fg} \omega_{AB}^{fg} + n_{AB}^{ff} \omega_{AB}^{ff} + n_{BB}^{gf} \omega_{BB}^{gf} \quad (1)$$

where  $n_A^f$  and  $n_B^f$  are the numbers of lipid chains of species A and B in a fluid state. The  $n_{\alpha\beta}^{ij}$  are the number of interactions between species  $\alpha$  and  $\beta$  in state  $i$  and  $j$ , respectively.

Four additional parameters are the melting enthalpies of the two species,  $\Delta H_A$  and  $\Delta H_B$ , and their melting entropies,  $\Delta S_A$  and  $\Delta S_B$ . These parameters can all be determined from the experimental melting profiles. In the Monte-Carlo procedure, a given number of lipids of species A and B is distributed randomly on a computer generated triangular lattice with periodic boundary conditions. Then, attempts are made to change the state of a randomly chosen lipid from fluid to gel or vice versa (Glauber steps). The likelihood of such an event to happen is given by a Boltzmann factor. Furthermore, diffusion is modeled by nearest neighbor exchange (Kawasaki steps). Details are given in [11,12,13].

## Theoretical considerations

During a Monte-Carlo simulation the membrane system fluctuates around the thermal equilibrium, e.g. each snapshot during the simulation displays a slightly different enthalpy. The fluctuations in enthalpy, however, are proportional to the heat capacity,  $c_p$ , via the relation [14]

$$c_p = \frac{\overline{H^2} - \overline{H}^2}{RT^2} \quad (2)$$

Similarly, fluctuations in volume yield the isothermal volume compressibility,  $\kappa_T^V$ , and fluctuations in area yield the isothermal area compressibility,  $\kappa_T^A$  [14]:

$$\kappa_T^V = \frac{\overline{V^2} - \overline{V}^2}{\overline{V} \cdot RT} \quad \text{and} \quad \kappa_T^A = \frac{\overline{A^2} - \overline{A}^2}{\overline{A} \cdot RT} \quad (3)$$

These relations are a consequence of the fluctuation-dissipation theorem [15,16], but can also be derived just from the derivatives of the statistical thermodynamics averages of  $H_i$ ,  $V_i$  and  $A_i$  ( $i$  denoting the different states of the system). According to Evans [17], the bending elasticity,  $\kappa_B$  (or the bending modulus,  $K_B = 1/\kappa_B$ ) of a membrane is related to the isothermal area compressibility via

$$\frac{1}{K_b} = \kappa_b = \frac{16 \cdot \kappa_T^A}{D^2} \quad , \quad (4)$$

where  $D$  is the membrane thickness (cf. [14]).

It has been shown experimentally that excess enthalpy changes,  $\Delta H$ , excess volume changes,  $\Delta V$ , and excess area changes,  $\Delta A$  during melting transitions are (within experimental error) exact proportional functions of the temperature ( $\Delta V(T) = \gamma_V \cdot \Delta H(T)$ ,  $\Delta A(T) = \gamma_A \cdot \Delta H(T)$ ). Therefore, enthalpy fluctuations, volume and area fluctuations are also proportional functions of the temperature.

Therefore, we obtain the following useful relations for changes of the elastic constants in melting transitions:

$$\Delta \kappa_T^V = \frac{\gamma_V^2 T}{V} \cdot \Delta c_p \quad , \quad (5)$$

$$\Delta \kappa_T^A = \frac{\gamma_A^2 T}{A} \cdot \Delta c_p \quad , \quad (6)$$

$$\Delta \kappa_B = \frac{16 \gamma_A^2 T}{D^2 A} \cdot \Delta c_p \quad , \quad (7)$$

where  $\gamma_V = 7.8 \cdot 10^{-4} \text{ cm}^3 / \text{J}$  and  $\gamma_A = 8.9 \cdot 10^3 \text{ cm}^2 / \text{J}$  are constants, roughly independent on the choice of the lipid [14,18].

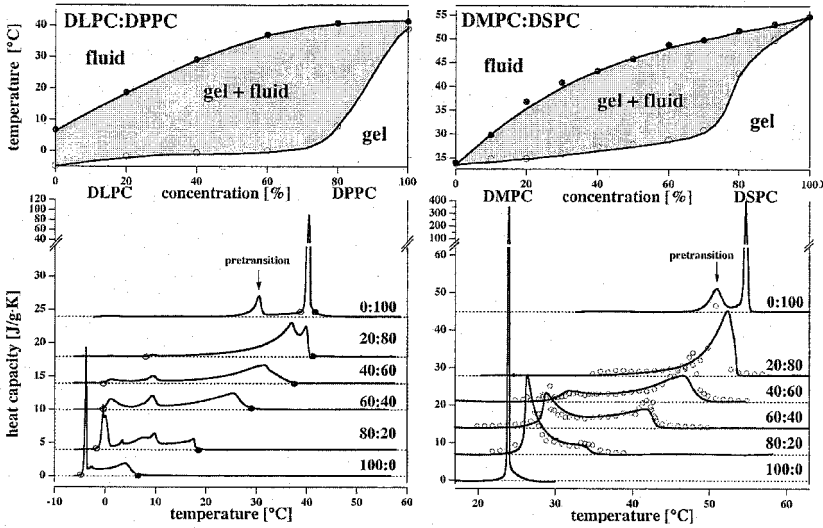


**Figure 1:** Left: Phase diagrams of DLPC-DPPC mixtures and the corresponding heat capacity profiles. The upper and lower phase boundaries have been obtained from the upper (●) and lower (○) limits of the  $c_p$ -profiles. Right: Phase diagram of DMPC-DSPC mixtures and the corresponding heat capacity profiles. Symbols (○) represent results from Monte-Carlo simulations. The phase coexistence regime is shaded in grey.

The fluctuations given in eqs. (2) and (3) are those of the whole lipid matrix, thus being macroscopic quantities. However, one can also define the fluctuations at each lattice point of the simulation by defining a state parameter  $S(i,j)$  for each lattice site, which may be either 0 or 1 for gel and fluid lipid state, respectively [13]. The degree of fluctuations at each lattice point can be determined during a Monte-Carlo simulation by determination of the mean square deviation of the parameter  $S(i,j)$ .

$$\text{local fluctuations} = \overline{S^2(i,j)} - \overline{S(i,j)}^2 \quad (8)$$

Fluctuations as defined in (8) may assume values between 0 and 0.25. Large local fluctuations are accompanied by increased elastic constants and reduced relaxation times [19]. Using Monte-Carlo simulations we show below that such local fluctuations are especially strong at domain interfaces, thus giving rise to distinctly different physical properties at the domain boundaries. Practically, in the simulation the local fluctuations were recorded such that diffusion steps were switched off after equilibration for some MC-cycles and the state fluctuations in a given lipid configuration were determined before switching diffusion on again.

## Results

### Phase behavior of binary lipid mixtures

In the following we will consider the phase behavior of binary lipid systems, in particular of DLPC:DPPC and DMPC:DSPC mixtures. We recorded heat capacity profiles at various molar ratios (Fig.1).

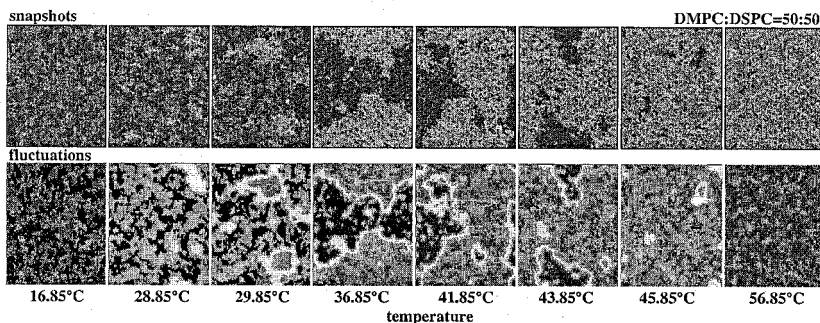


**Figure 2:** Lipid state distribution and fluctuations of a DMPC:DSPC=50:50 mixture in the chain melting regime as a function of temperature (from Monte-Carlo simulations). **Top:** Snapshots at different temperatures with a simulation box of  $80 \times 80$  lipid chains. The two dark grey shades correspond to gel state lipid chains of DMPC and DSPC, respectively. The two light grey shades correspond to the fluid states of DMPC and DSPC. **Bottom:** Fluctuations of the lipid matrices in the top panels, as defined in eq. 8. Brighter shades correspond to larger fluctuations. Fluctuations are largely enhanced at the domain interfaces.

A common procedure to generate phase diagrams is to identify phase boundaries from a tangent construction at the lower and upper limits of the heat capacity profiles. These values are plotted into a temperature versus concentration graph. This is an empirical method that does not guarantee that these temperature limits are the correct phase boundaries. If phase separation occurs, the composition of the macroscopic phases is well defined. Under such a condition, from confocal microscopy determination of domain sizes as a function of temperature and composition one can draw phase diagrams that relate the position in phase space with fraction of each phase and its composition, and compare it to calorimetric measurements.

Heat capacity profiles can also be simulated with reasonable accuracy using Monte-Carlo simulations as described above (see [11,12,13], cf. Fig. 1, right). Snapshots produced in such simulations (Fig. 2) can be used to arrive at a deeper understanding of the processes

that result in domain formation, and they can be compared to confocal microscopy images (Fig. 3). Fig. 2 (top row) shows how domains form as a function of temperature in the DMPC:DSPC=50:50 mixture. At temperatures close to the outer heat capacity maxima ( $\sim 29^\circ\text{C}$  and  $\sim 44^\circ\text{C}$ , respectively, cf. Fig. 4), gel and fluid domains are smaller than system size. In the intermediate temperature regime domains become macroscopic (only one large gel and fluid domain – note the periodic boundary conditions).

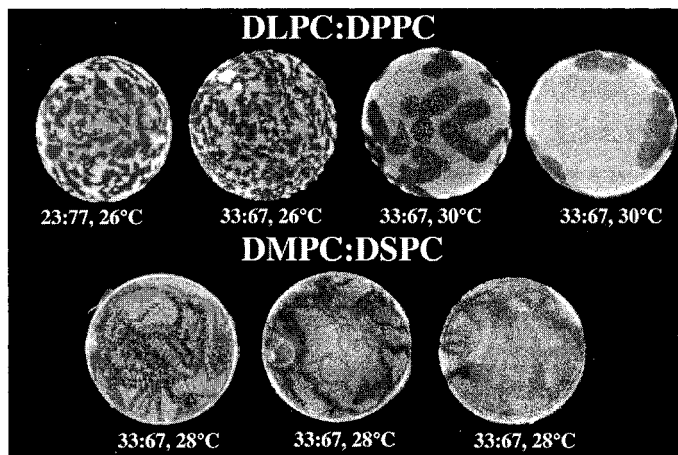


**Figure 3:** Confocal microscopy images of giant vesicles of DLPC-DPPC and DMPC-DSPC mixtures at different mixing ratios and temperatures. Domain sizes and shapes vary considerably, dependent on experimental conditions. Dark regions correspond to gel domains. Vesicular sizes range from 20 to 30  $\mu\text{m}$ .

Within each phase, however, one can still notice small domains of the opposite chain state, which fluctuate during simulation time. Even in the gel phase at low ( $16.85^\circ\text{C}$ ) and the fluid phase at high ( $56.85^\circ\text{C}$ ) temperatures one can recognize local segregation of the two lipids into two types of gel or fluid domains, respectively. The bottom row of Fig. 2 shows the local fluctuations (eq. 8) corresponding to the snapshots in the top row. It can be clearly seen that they occur predominantly at the domain interfaces. Remember that highly fluctuating regions will display the highest elasticity and compressibility. The simulations shown here do not contain out-of-plane degrees of freedom. However, in coupled bilayers curvature modes can in principle be obtained by considering the local area differences on both monolayers. This concept has successfully been used by Heimburg [20] to obtain a consistent thermodynamical picture of the formation of the ripple phase. By looking at the temperature progression of the fluctuations (Fig. 2) one can well see that domain formation is not the only property that describes the physics of the system but that there



are also large fluctuations in particular in temperature regimes of high heat capacity, which not necessarily coincide with regions of large domain formation. Those are the most interesting regimes.

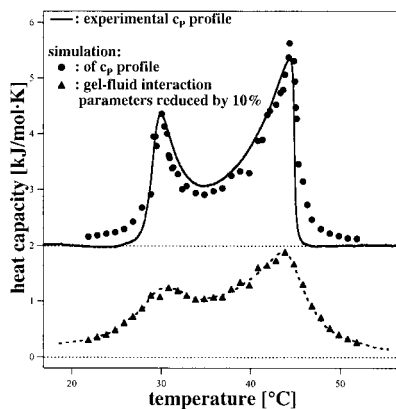


**Figure 4: Top:** Experimental heat capacity profile of a 50:50 DMPC:DSPC mixture (solid line) and the corresponding Monte-Carlo simulation (symbols). **Bottom:** Simulation of the same mixture using gel-fluid interaction parameters,  $\omega_{\alpha\beta}^{gf}$ , being only 90% of those used to simulate the top trace.

Confocal microscopy images of lipid mixtures demonstrate that subtle changes in temperature can alter the vesicles from forming domains smaller than vesicular size (DLPC:DPPC=33:67, 26°C) to vesicles displaying large domains (DLPC:DPPC=33:67, 30°C). Gel and fluid domain areas deviate from the values obtained by applying the lever rule to the phase diagram in Fig.1 (left).

In simulations it can be shown that the criteria for whether a system displays microscopic domains or macroscopic domains (that grow with system size) depends in a delicate manner on the interaction between lipids (Fig. 4 and Fig. 5). The size and shape of domains is dominated by nearest neighbor interactions in the lipid matrix. Fig. 4 shows that the melting profiles of a DMPC:DSPC=50:50 (top trace) mixture is slightly broadened upon reduction of the gel-fluid interactions by 10% (bottom trace) in the simulation. The consequences for the domain pattern, however, are dramatic. Fig.5 shows Monte-Carlo snapshots for varying matrix sizes (30×30, 60×60, 120×120 and 180×180 chains) for the two cases in Fig.4 at  $T=36.85^\circ\text{C}$ . The parameters that describe the experimental profiles well (top trace in Fig. 4) lead to macroscopic phase separation (Fig.5, left top), evident in the separation into one large gel and one large fluid domain, independent of matrix size.

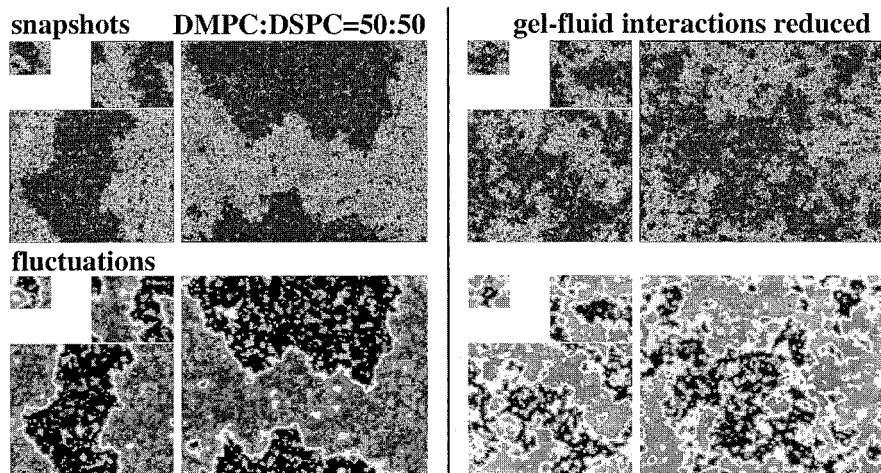


**Figure 5:** Simulation snapshots for various matrix sizes:  $30 \times 30$ ,  $60 \times 60$ ,  $120 \times 120$  and  $180 \times 180$  lipid chains. **Left, top:** Snapshots corresponding to the heat capacity curve of the DMPC:DSPC=50:50 mixture at  $36.9^\circ\text{C}$  (upper  $c_p$ -profile of Fig. 4), showing macroscopic phase separation into fluid and gel independent of matrix size. **Left, bottom:** Corresponding local fluctuations. **Right, top:** Snapshots corresponding to the bottom  $c_p$  trace of Fig.5 at  $36.85^\circ\text{C}$ , showing that domains are smaller than the matrix size on all length scales if the interfacial tension at the gel-fluid domain boundaries are reduced. **Right, bottom:** Corresponding fluctuations, showing pronounced differences in the fluctuations as compared to the case in the left hand panels.

The fluctuations in this system are large at the domain interfaces (white regions in Fig.5, left, bottom). Increasing matrix size leads to a relative reduction of the fraction of the fluctuating interface. Interestingly, the two phases themselves display different fluctuation strength (evident from different shades of grey in the bottom panels of Fig.5). If the gel-fluid nearest neighbor interactions are reduced by 10% in the simulation (as it could be done experimentally by adding small molecules like local anesthetics), the differences in domain shape are profound (Fig.5, right). Domain formation now occurs on all length scales and there are no obvious dependencies on matrix size. Although we did not perform correlation length analysis, this can in principle be done by using pair correlation functions [21] or by calculating the structure factor of the lipid matrix [22]. The composition of each domain fluctuates and is not well defined as compared to macroscopic phase separation (Fig.5, left). It is unlikely that confocal microscopy would be able to correctly determine gel and domain areas. One cannot consider these systems as phase separated because on all length scales coexistence of the two lipid states is found. The lipid matrix is to a much

larger degree dominated by fluctuating interfaces as compared to the left hand panels of Fig.5. This effect is even more pronounced if the gel-fluid interactions are reduced by 20% (not shown), where the large-scale domain structure nearly completely dissolves and the whole matrix is dominated by fluctuations. As mentioned, such changes can among other factors be induced by addition of small molecules, which broaden  $c_p$ -profiles and thus reduce the interfacial tension at domain boundaries (cf. 13).

## Conclusions

Here, we present “phase diagrams” of lipid mixtures derived from calorimetry and critically discuss the implications of a statistical thermodynamics analysis of the heat capacity profiles. Clearly, the reduction of domain length scales induced by reduction of the interaction parameters (interfacial tension at the domain boundaries) leads to larger fluctuations of the lipid systems in the melting regime. No defined physical property (e.g. defined concentration of components, or order parameter) can be attributed to the individual domains. Thus, the concept of phase separation starts failing if the domains become small. This is caused by the fact that the lipid matrix starts to be dominated by domain interfaces and their fluctuations, which do not have an equivalent in a picture consisting exclusively of coexisting phases. In respect to the ongoing discussion of the physical nature of “rafts” in biomembranes, it is likely that small domains (or rafts) will be subject to large fluctuations. In a recent review by Simons and Vaz [6] the authors argue *“There is no fundamental requirement that any phase in a heterogeneous system not be divided into several part or domains, although their exact thermodynamic description becomes unreliable when the domains become too small”*. In our view the first part of this statement is incorrect, while the second one is clearly true. This is the case because the fluctuations at the domains interfaces enter into the physical picture.

- [1] E. Sackmann, in: *Structure and Dynamics of Membranes: From Cells to Vesicles*, Elsevier **1995**
- [2] A. G. Lee, *Biochim.Biophys. Acta* **1977**, 472, 285
- [3] H. M. McConnell, D. J. Keller, *Proc.Natl.Acad.Sci.USA* **1987**, 84, 4706
- [4] J. Korlach, P. Schwille, W. W. Webb, G. W. Feigenson, *Proc.Natl.Acad.Sci.USA* **1999**, 96, 8461
- [5] L. A. Bagatolli and E. Gratton, *Biophys. J.* **1999**, 77, 2090
- [6] K. Simons, W. L. C. Vaz, *Annu.Rev.Biomol.Struct.* **2004**, 33, 269
- [7] H. Heerklotz, *Biophys.J.* **2002**, 83, 2693
- [8] T. Baumgartl, S. T. Hess, W. W. Webb, *Nature* **2003**, 425, 821
- [9] V. P. Ivanova, T. Heimburg, *Phys Rev. E* **2001**, 63, 1914
- [10] M. I. Angelova, S. Soléau, P. Méléard, J. F. Faucon, P. Bothorel, *Progr. Colloid. Polym. Sci.* **1992**, 89, 127
- [11] I. P. Sugar, T. E. Thompson, R. L. Biltonen, *Biophys. J.* **1999**, 76, 2099
- [12] A. E. Hac, H. Seeger, M. Fidorra, T. Heimburg, *Biophys. J.* **2004**, submitted
- [13] V. P. Ivanova, I. Makarov, T. E. Schäffer, T. Heimburg, *Biophys. J.* **2003**, 84, 2427
- [14] T. Heimburg, *Biochim. Biophys. Acta* **1998**, 1415, 147
- [15] H. B. Callen, R. F. Green, *Phys. Rev.* **1952**, 86, 702
- [16] R. Kubo, *Rep. Prog. Phys.* **1966**, 29, 255
- [17] E. A. Evans, *Biophys. J.* **1974**, 14, 923
- [18] H. Ebel, P. Grabitz, T. Heimburg, *J. Phys. Chem. B* **2001**, 105, 7353
- [19] P. Grabitz, V. P. Ivanova, T. Heimburg, *Biophys. J.* **2002**, 82, 299
- [20] T. Heimburg, *Biophys. J.* **2000**, 78, 1154
- [21] K. Jørgensen, M. M. Sperotto, O. G. Mouritsen, J. H. Ipsen, M. J. Zuckermann, *Biochim. Biophys. Acta* **1993**, 1152, 135
- [22] L. K. Nielsen, T. Bjørnholm, O. G. Mouritsen, *Nature* **2000**, 404, 352